Inorg. Chem. **2008**, *47*, 10626−10633

High Resolution Mass Spectrometry for Studying the Interactions of Cisplatin with Oligonucleotides

Alexander E. Egger,[†,‡] Christian G. Hartinger,[*,†,‡] Hisham Ben Hamidane,[‡] Yury O. Tsybin,[‡] Bernhard K. Keppler,[†] and Paul J. Dyson[‡]

University of Vienna, Institute of Inorganic Chemistry, Waehringer Str. 42, A-1090 Vienna, Austria, and Institut des Sciences et Ingénierie Chimiques, Ecole Polytechnique Fédérale de Lausanne (EPFL), CH-1015 Lausanne, Switzerland

Received July 22, 2008

Fourier transform ion cyclotron resonance mass spectrometry (FT-ICR MS) has been used to probe the interaction of the anticancer drug cisplatin with oligonucleotides. The binding kinetics, the nature of the adducts formed, and the location of the binding site within the specifically designed double-stranded DNA oligonucleotides, ds(GTAT-TGGCACGTA) and ds(GTACCGGTGTGTA), were determined by recording mass spectra over time and/or employing tandem mass spectrometry (MS/MS). The FT-ICR MS studies show that binding to DNA takes place via a $[Pt(NH_3)_2Cl]^+$ intermediate prior to formation of bifunctional $[Pt(NH_3)_2]^{2+}$ adducts. Tandem MS reveals that the major binding sites correspond to GG and GTG, the known preferred binding sites for cisplatin, and demonstrates the preference for binding to guanosine within the oligonucleotide. The obtained results are discussed and compared to published data obtained by other mass spectrometric techniques, NMR spectroscopy and X-ray crystallography.

Introduction

Platinum complexes such as cisplatin, carboplatin, and oxaliplatin (Figure 1) are widely used drugs for the treatment of cancer.[1] DNA is generally accepted to be the critical target for platinum-based compounds,[2] which induce structural modifications on the helix, that ultimately lead to apoptosis.[1] It has been shown that cisplatin binds to the purine-*N*7 of DNA bases in cell free media, mainly causing intrastrand adducts between adjacent guanine residues (pGpG) or neighboring adenine and guanine residues (pApG) as well as interstrand adducts and monoadducts.[3−5] These binding interactions have been confirmed in vivo by analysis of leukocytes extracted from venous blood of cisplatin-treated patients. The adducts were characterized as mainly pGpG intrastrand cross-links (65%), followed by pApG intrastrand cross-links (22%), interstrand and/or intrastrand cross-links on pGpXpG sequences (13%) and monofunctional adducts (<1%).[6] Notably, the treatment response of cancer patients suffering from ovarian or testicular cancer has been correlated to the level of intrastrand adducts formed.[7−9]

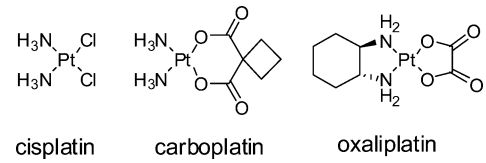

Figure 1. Structures of Pt compounds in worldwide clinical use for the treatment of various cancers.

Many different techniques have been used to characterize the interaction of metallodrugs with DNA, including NMR spectroscopy, capillary electrophoresis (CE), high-performance liquid chromatography (HPLC), X-ray diffraction

* To whom correspondence should be addressed. E-mail: christian.hartinger@univie.ac.at.
† University of Vienna.
‡ Ecole Polytechnique Fédérale de Lausanne (EPFL).

(1) Lippert, B. *Cisplatin: Chemistry and Biochemistry of a Leading Anticancer Drug*, 1st ed.; Helvetica Chimica Acta/Wiley-VCH: Zürich/Weinheim, 1999; p 576.
(2) Jamieson, E. R.; Lippard, S. J. *Chem. Rev.* **1999**, *99*, 2467–2498.
(3) Eastman, A. *Biochemistry* **1985**, *24*, 5027–5032.
(4) Eastman, A. *Biochemistry* **1986**, *25*, 3912–3915.
(5) Gupta, R.; Beck, J. L.; Sheil, M. M.; Ralph, S. F. *J. Inorg. Biochem.* **2005**, *99*, 552–559.
(6) Fichtinger-Schepman, A. M.; van Oosterom, A. T.; Lohman, P. H.; Berends, F. *Cancer Res.* **1987**, *47*, 3000–3004.
(7) Poirier, M. C.; Reed, E.; Zwelling, L. A.; Ozols, R. F.; Litterst, C. L.; Yuspa, S. H. *Environ. Health Perspect.* **1985**, *62*, 89–94.
(8) Reed, E.; Yuspa, S. H.; Zwelling, L. A.; Ozols, R. F.; Poirier, M. C. *J. Clin. Invest.* **1986**, *77*, 545–550.
(9) Reed, E.; Ozols, R. F.; Tarone, R.; Yuspa, S. H.; Poirier, M. C. *Proc. Natl. Acad. Sci. U. S. A.* **1987**, *84*, 5024–5028.

10.1021/ic801371r CCC: $40.75
Published on Web 10/24/2008

analysis and mass spectrometry.[6,10−17] NMR spectroscopy, mass spectrometry and X-ray diffraction have proven to be the most useful for the structural characterization[2] of nucleotide- and other DNA model-Pt complex adducts, as reported for cisplatin,[18−23] and other platinum complexes.[13,17,24,25] CE and HPLC are mainly used for determining binding kinetics for the reaction of complexes with nucleotides, sometimes in combination with MS characterization.[13,26−35] Mass spectrometric methods, based on different ionization sources and analyzers, have emerged as important tools in (bio)analytical studies especially when coupled to modern separation techniques.[14,15,34−40] In recent years, the interaction of cisplatin and other antitumor drug candidates with proteins, being the first potential interaction partners in the blood stream after intravenous administration, has been studied using various MS methods.[37,41−45] The transport proteins in human serum such as transferrin and albumin are of interest with regard to drug delivery, but also smaller proteins, such as cytochrome-c, glutathione *S*-transferase, and ubiquitin, have been studied to provide mechanistic information.[15,39,46−52]

Fourier transform ion cyclotron resonance mass spectrometry (FT-ICR MS) is unrivaled in terms of mass resolution and accuracy,[53] and ideally suited for studying the interaction of metallodrugs with biomolecules.[39,54] The reaction of anticancer drugs with proteins allows unambiguous characterization of the adducts based on MS/MS,[54] including, for example, binding site determination of cisplatin, transplatin, and oxaliplatin on ubiquitin.[39] To the best of our knowledge, FT-ICR MS has not previously been used to study interactions between metal drugs and oligonucleotides, or to determine the binding site of metallodrugs on an oligonucleotide using a top-down approach. In this report, the application of FT-ICR MS to probe the interactions of cisplatin with double-stranded DNA oligonucleotides is presented, and the results are compared to X-ray crystallography, NMR spectroscopic, and other mass spectrometric data from the literature.

Experimental Section

Chemicals and Sample Preparation. HPLC-purified double-stranded 13-mer oligonucleotides (ds(5′GTATTGGCACGTA) - ds1, and ds(5′GTACCGGTGTGTA) - ds2, see Table 1 for details) were obtained as 0.2 mM aqueous solutions from A/S Technology

(10) Beck, J. L.; Colgrave, M. L.; Kapur, A.; Iannitti-Tito, P.; Ralph, S. F.; Sheil, M. M.; Weimann, A.; Wickham, G. *Adv. Mass Spectrom.* **2001**, *15*, 175–192.
(11) Beck, J. L.; Colgrave, M. L.; Ralph, S. F.; Sheil, M. M. *Mass Spectrom. Rev.* **2001**, *20*, 61–87.
(12) Koomen, J. M.; Ruotolo, B. T.; Gillig, K. J.; McLean, J. A.; Russell, D. H.; Kang, M.; Dunbar, K. R.; Fuhrer, K.; Gonin, M.; Schultz, J. A. *Anal. Bioanal. Chem.* **2002**, *373*, 612–617.
(13) Hartinger, C. G.; Schluga, P.; Galanski, M.; Baumgartner, C.; Timerbaev, A. R.; Keppler, B. K. *Electrophoresis* **2003**, *24*, 2038–2044.
(14) Hartinger, C. G.; Keppler, B. K. *Electrophoresis* **2007**, *28*, 3436–3446.
(15) Hartinger, C. G.; Ang, W. H.; Casini, A.; Messori, L.; Keppler, B. K.; Dyson, P. J. *J. Anal. At. Spectrom.* **2007**, *22*, 960–967.
(16) Dorcier, A.; Hartinger, C. G.; Scopelliti, R.; Fish, R. H.; Keppler, B. K.; Dyson, P. J. *J. Inorg. Biochem.* **2008**, *102*, 1066–1076.
(17) Kerr, S. L.; Shoeib, T.; Sharp, B. L. *Anal. Bioanal. Chem.* **2008**, *391*, 2339–2348.
(18) Sherman, S. E.; Gibson, D.; Wang, A. H. J.; Lippard, S. J. *Science* **1985**, *230*, 412–417.
(19) Sherman, S. E.; Gibson, D.; Wang, A. H. J.; Lippard, S. J. *J. Am. Chem. Soc.* **1988**, *110*, 7368–7381.
(20) van Garderen, C. J.; van Houte, L. P. A. *Eur. J. Biochem.* **1994**, *225*, 1169–1179.
(21) Takahara, P. M.; Rosenzweig, A. C.; Frederick, C. A.; Lippard, S. J. *Nature* **1995**, *377*, 649–652.
(22) Huang, H.; Zhu, L.; Reid, B. R.; Drobny, G. P.; Hopkins, P. B. *Science* **1995**, *270*, 1842–1845.
(23) Takahara, P. M.; Frederick, C. A.; Lippard, S. J. *J. Am. Chem. Soc.* **1996**, *118*, 12309–12321.
(24) Ano, S. O.; Intini, F. P.; Natile, G.; Marzilli, L. G. *J. Am. Chem. Soc.* **1998**, *120*, 12017–12022.
(25) Komeda, S.; Moulaei, T.; Woods, K. K.; Chikuma, M.; Farrell, N. P.; Williams, L. D. *J. Am. Chem. Soc.* **2006**, *128*, 16092–16103.
(26) Da Col, R.; Silvestro, L.; Baiocchi, C.; Giacosa, D.; Viano, I. *J. Chromatogr.* **1993**, *633*, 119–128.
(27) Reeder, F.; Guo, Z.; Murdoch, P. D. S.; Corazza, A.; Hambley, T. W.; Berners-Price, S. J.; Chottard, J.-C.; Sadler, P. J. *Eur. J. Biochem.* **1997**, *249*, 370–382.
(28) Zenker, A.; Galanski, M.; Bereuter, T. L.; Keppler, B. K.; Lindner, W. *J. Chromatogr. A* **1999**, *852*, 337–346.
(29) Strickmann, D. B.; Küng, A.; Keppler, B. K. *Electrophoresis* **2002**, *23*, 74–80.
(30) Volckova, E.; Dudones, L. P.; Bose, R. N. *Pharm. Res.* **2002**, *19*, 124–131.
(31) Hartinger, C. G.; Timerbaev, A. R.; Keppler, B. K. *Electrophoresis* **2003**, *24*, 2023–2037.
(32) Galanski, M.; Baumgartner, C.; Meelich, K.; Arion, V. B.; Fremuth, M.; Jakupec, M. A.; Schluga, P.; Hartinger, C. G.; von Keyserlingk, N. G.; Keppler, B. K. *Inorg. Chim. Acta* **2004**, *357*, 3237–3244.
(33) Warnke, U.; Rappel, C.; Meier, H.; Kloft, C.; Galanski, M.; Hartinger, C. G.; Keppler, B. K.; Jaehde, U. *ChemBioChem* **2004**, *5*, 1543–1549.
(34) Groessl, M.; Hartinger, C. G.; Dyson, P. J.; Keppler, B. K. *J. Inorg. Biochem.* **2008**, *102*, 1060–1065.
(35) Groessl, M.; Hartinger, C. G.; Połeć-Pawlak, K.; Jarosz, M.; Keppler, B. K. *Electrophoresis* **2008**, *29*, 2224–2232.
(36) Szpunar, J. *Analyst* **2005**, *130*, 442–465.
(37) Timerbaev, A. R.; Hartinger, C. G.; Aleksenko, S. S.; Keppler, B. K. *Chem. Rev.* **2006**, *106*, 2224–2248.
(38) Will, J.; Kyas, A.; Sheldrick, W. S.; Wolters, D. *J. Biol. Inorg. Chem.* **2007**, *12*, 883–894.
(39) Hartinger, C. G.; Tsybin, Y. O.; Fuchser, J.; Dyson, P. J. *Inorg. Chem.* **2008**, *47*, 17–19.
(40) Will, J.; Sheldrick, W. S.; Wolters, D. *J. Biol. Inorg. Chem.* **2008**, *13*, 421–434.
(41) Allardyce, C. S.; Dyson, P. J.; Coffey, J.; Johnson, N. *Rapid Commun. Mass Spectrom.* **2002**, *16*, 933–935.
(42) Pongratz, M.; Schluga, P.; Jakupec, M. A.; Arion, V. B.; Hartinger, C. G.; Allmaier, G.; Keppler, B. K. *J. Anal. At. Spectrom.* **2004**, *19*, 46–51.
(43) Khalaila, I.; Allardyce, C. S.; Verma, C. S.; Dyson, P. J. *ChemBioChem* **2005**, *6*, 1788–1795.
(44) Khalaila, I.; Bergamo, A.; Bussy, F.; Sava, G.; Dyson, P. J. *Int. J. Oncol.* **2006**, *29*, 261–268.
(45) Groessl, M.; Reisner, E.; Hartinger, C. G.; Eichinger, R.; Semenova, O.; Timerbaev, A. R.; Jakupec, M. A.; Arion, V. B.; Keppler, B. K. *J. Med. Chem.* **2007**, *50*, 2185–2193.
(46) Gibson, D.; Costello, C. E. *Eur. Mass Spectrom.* **1999**, *5*, 501–510.
(47) Peleg-Shulman, T.; Gibson, D. *J. Am. Chem. Soc.* **2001**, *123*, 3171–3172.
(48) Peleg-Shulman, T.; Najajreh, Y.; Gibson, D. *J. Inorg. Biochem.* **2002**, *91*, 306–311.
(49) Ang, W. H.; Khalaila, I.; Allardyce, C. S.; Juillerat-Jeanneret, L.; Dyson, P. J. *J. Am. Chem. Soc.* **2005**, *127*, 1382–1383.
(50) Casini, A.; Mastrobuoni, G.; Ang, W. H.; Gabbiani, C.; Pieraccini, G.; Moneti, G.; Dyson, P. J.; Messori, L. *ChemMedChem* **2007**, *2*, 631–635.
(51) Scolaro, C.; Chaplin, A. B.; Hartinger, C. G.; Bergamo, A.; Cocchietto, M.; Keppler, B. K.; Sava, G.; Dyson, P. J. *Dalton Trans.* **2007**, 5065–5072.
(52) Casini, A.; Hartinger, C. G.; Gabbiani, C.; Mini, E.; Dyson, P. J.; Keppler, B. K.; Messori, L. *J. Inorg. Biochem.* **2008**, *102*, 564–575.
(53) Marshall, A. G.; Hendrickson, C. L.; Emmett, M. R.; Rodgers, R. P.; Blakney, G. T.; Nilsson, C. L. *Eur. J. Mass Spectrom.* **2007**, *13*, 57–59.
(54) Weidt, S. K.; Mackay, C. L.; Langridge-Smith, P. R. R.; Sadler, P. J. *Chem. Commun.* **2007**, 1719–1721.

Table 1. Primary Structure of Four Single-Stranded Oligonucleotides (S1, S1c, S2 and S2c), Forming Two Double-Stranded Oligonucleotides (ds1 and ds2)

	oligonucleotide	mass (g/mol)
ds1	5′HO-GTATTGGCACGTA-OH3′ (S1)	3989.6
	5′HO-TACGTGCCAATAC-OH3′ (S1c)	3918.6
ds2	5′HO-GTACCGGTGTGTA-OH3′ (S2)	4005.6
	5′HO-TACACACCGGTAC-OH3′ (S2c)	3903.6

(Denmark) and checked by PAGE (20%), followed by ethidium bromide staining, for complete annealing and homogeneity upon delivery.[55] The migration behavior of the double strands was compared to the respective single strands.

Ammonium acetate (>99.99%) and cisplatin were purchased from Sigma-Aldrich (Buchs, Switzerland), and HPLC-grade solvents (water, methanol, and *n*-propanol) from Acros (Beel, Belgium).

To study the binding kinetics of cisplatin toward the oligonucleotides, cisplatin was freshly dissolved in water and incubated in Eppendorf tubes with the respective double-stranded oligonucleotide in an effective complex/oligonucleotide ratio of 60:20 μM for up to 50 h at 37 °C in a thermomixer at 300 rpm in the dark. Evaporation was minimized by sealing the tubes with parafilm. Aliquots of 30 μL were taken after 0.25, 1, 3, 6, 15, 21, and 50 h and stored at −20 °C until analysis by mass spectrometry.

Nanoelectrospray Ionization Fourier Transform Ion Cyclotron Resonance Mass Spectrometry (nESI FT-ICR MS). In order to minimize exposure of DNA to high concentrations of organic solvents, which are essential for stable spraying, aqueous samples were thawed and diluted immediately prior to analysis 1:10 with a 1.1 mM solution of ammonium acetate in water/*n*-propanol/methanol giving a ratio of 30/5/65 and a final DNA concentration of 2 μM.

For electrospray ionization mass spectrometry, the samples were placed into a 96-well plate in an Advion TriVersa robot (Advion Biosciences, Ithaca, NY) equipped with a 5.5 μm-nozzle chip. The ESI robot was controlled with ChipSoft v7.2.0 software employing the following parameters: gas pressure 0.40 psi; voltage 1.8−2.0 kV; sample volume 10 μL. The samples were analyzed in negative ion mode using a hyphenated ion-trap-FT-ICR mass spectrometer comprising an LTQ XL and an 11 T FT-ICR MS (both ThermoFisher Scientific, Bremen, Germany). The Xcalibur software bundle was utilized for data acquisition (Tune Plus version 2.2 SP1; ThermoFisher Scientific) and data analysis (Qual Browser version 2.2; ThermoFisher Scientific).

Mass spectra were recorded at a resolution of 75000 at 500 *m*/*z* for *m*/*z* 350−2000 and 400−1500 for full spectra and MS/MS, respectively. One scan consisted of 5 microscans and the spectrum was averaged over at least 50 scans. For tandem MS analysis, the most abundant charge state of the $[Pt(NH_3)_2]^{2+}$ adduct peak was fragmented by collision induced dissociation (CID) in the linear ion trap with subsequent product ion transfer into the ICR cell for high resolution detection and infrared multiphoton dissociation (IRMPD), performed directly in the ICR cell using 10.6 μm CO_2 laser. The experimental parameters are summarized in Table 2.

Data Analysis. XCalibur software (version 2.0.5) was applied for offline recalibration of the recorded full-spectra, using the charge distributions (4−9-fold negatively charged, see Supporting Information) of a single-stranded, unplatinated oligonucleotide, improving mass-accuracy from approximately 2 ppm to <1 ppm for nearly all identified peaks. The full spectra recorded for the kinetic study

Table 2. Instrument Parameters for the FT-ICR MS Experiments

		MS/MS	
	Full MS	IRMPD	CID
AGC	1×10^6	5×10^5	5×10^5
max injection time (ms)	500	1000	1000
isolation width (*m*/*z*)		5	5

were deconvoluted using ProMass (ThermoFisher Scientific). For semiquantitative analysis of the binding kinetics, the charge state exhibiting equal intensities of the two corresponding unmodified single strands was chosen. Relative peak intensities, normalized to the highest peak of the investigated charge state, were plotted against the incubation time with ds1 or ds2. For MS^2 data analysis, at least two assignable unplatinated fragments, being present in both the IRMPD and CID spectra, were used for offline recalibration (see Supporting Information, Table S1). Routinely, all signals with an intensity of >1% were selected for interpretation and for platinum free fragments the web-based Mongo Oligo Mass calculator v2.06 (http://library.med.utah.edu/masspec/mongo.htm) was used for assignments.[56] The platinum containing adducts could be unambiguously identified by their characteristic isotopic distributions (Figure 2, top) as well as by the formation of a daughter peak due to the loss of an ammine ligand. The $[Pt(NH_3)_2]^{2+}$ (or $[Pt(NH_3)]^{2+}$) adduct was subtracted and the resulting platinum-free mass of the oligonucleotide was identified with the Mongo Oligo Mass calculator. Additionally, theoretical and measured isotopic patterns for all identified Pt-containing fragments were compared and their mass accuracy was calculated.

Results and Discussion

Cisplatin is known to bind primarily to the *N*7 of guanine residues, especially when two guanine moieties occupy adjacent position on the DNA strand. More generally, it has been reported that TGGC is the preferred DNA binding sequence for transition metals.[57] Therefore, an oligonucleotide (termed ds1) was designed with the preferred Pt binding site (GG) embedded within a TGGC sequence, with the complementary strand comprising a binding site of secondary importance (GTG). A second oligonucleotide (termed ds2) contained the TGGC binding site in both strands (see Table 1).

nESI FT-ICR MS Spectra of Oligonucleotides. Spectra of the investigated 13-mer double-stranded oligonucleotides (ds1 and ds2) were recorded in negative ion mode and detected as their corresponding single-stranded oligonucleotides (S1/S1c and S2/S2c) with charge states between −4 and −9. Unplatinated S1c or S2c were used for offline internal recalibration. Separation of the double-stranded oligonucleotides into their complementary single strands was always observed, irrespective of the degree of platination, the spraying conditions and the solvent composition (concentration of organic solvent, use of buffer or pure water, etc.), as expected for the chosen system.[58−60] Strand separation facilitates the interpretation of tandem mass spectra since

(55) Sambrook, J.; Russel, D. W. *Molecular cloning - A laboratory manual*, 3rd ed.; Cold Spring Harbor Laboratory Press: New York, 2001; Vol. *1*, pp 5.40−45.46.

(56) Ni, J.; Pomerantz, S. C.; Rozenski, J.; Zhang, Y.; McCloskey, J. A. *Anal. Chem.* **1996**, *68*, 1989–1999.

(57) Bregadze, V. G. Metal ion interactions with DNA: considerations on structure, stability, and effects from metal ion binding. In *Metal Ions in Biological Systems*; Sigel, A.; Sigel, H., Eds.; Marcel Dekker: New York, 1996; Vol. *32*, pp 419−451.

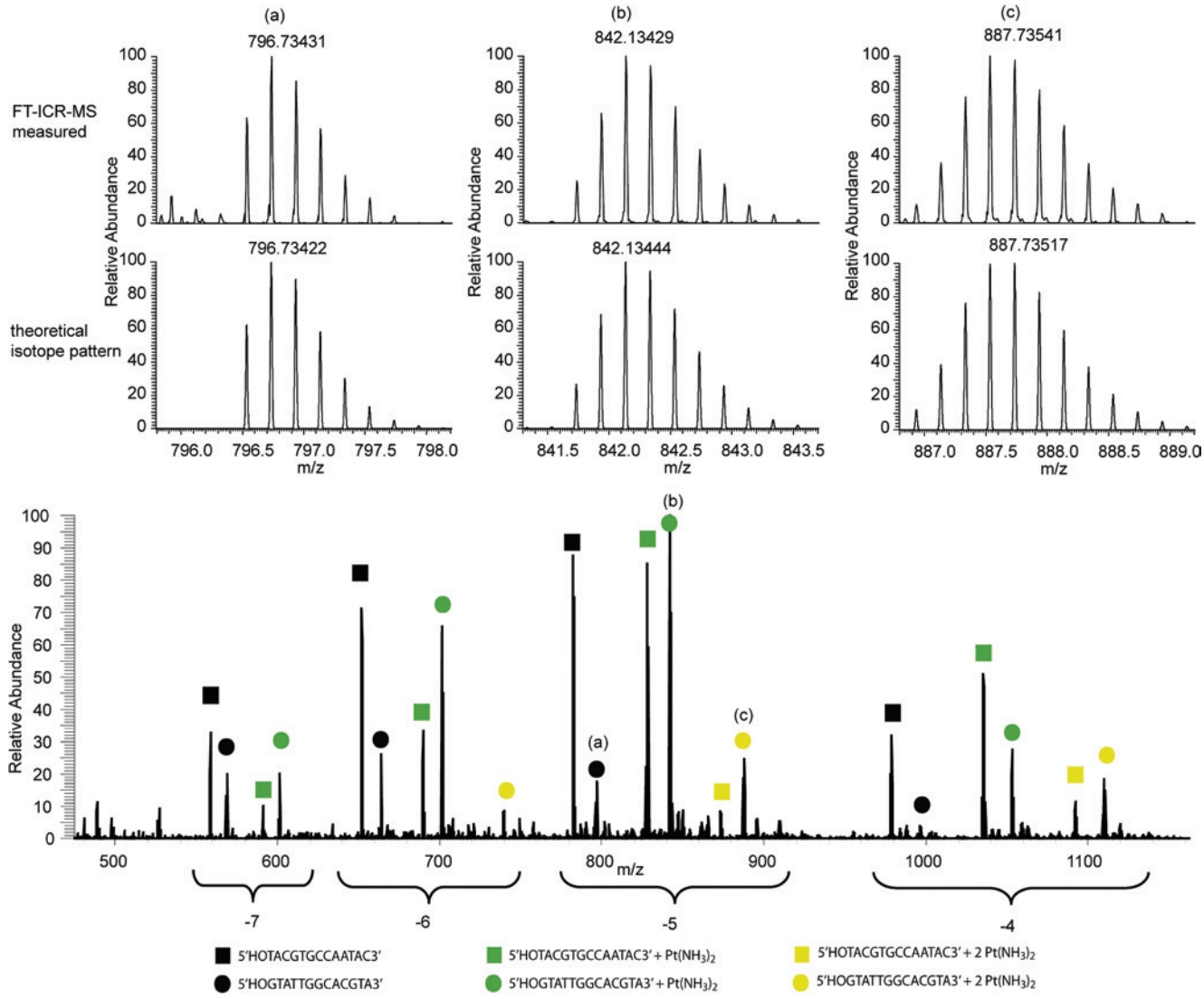

Figure 2. FT-ICR mass spectrum of ds(5′HOGTATTGGCACGTA3′) (ds1), incubated with cisplatin for 50 h with an oligonucleotide/Pt ratio of 1:3 (bottom). Effective spraying conditions (1 mM ammonium acetate and 2 μM oligonucleotide in methanol/water/*n*-propanol = 65:30:5) lead to negatively charged species and a complete separation of the double-stranded oligonucleotide into corresponding single strands (■ and ●). The experimental and theoretical peak patterns of unplatinated single-stranded oligonucleotide (a), the $Pt(NH_3)_2$ adduct (b), and the bis-$Pt(NH_3)_2$ adduct (c) are shown.

the adducts could be assigned to one of the strands. The FT-ICR mass spectrum for a 50 h incubation of ds1 with cisplatin is shown in Figure 2 together with details of the experimentally observed signals and corresponding theoretical patterns for unplatinated single-stranded species $[S1 - 5H]^{5-}$ at *m/z* 796.73431, singly platinated $[S1 + Pt(NH_3)_2 - 7H]^{5-}$ at *m/z* 842.13429 and doubly platinated $[S1 + 2Pt(NH_3)_2 - 9H]^{5-}$ at *m/z* 887.73541. Because of the characteristic isotope distribution of platinum, the Pt-free, singly and doubly platinated oligonucleotide signals can easily be distinguished (Figure 2).

The relative intensities of S1 and S1c are dependent on the charge state: when analyzing the unplatinated oligomer ds1, the peaks assigned to S1 are more intense than S1c for charge states ≥ -7, whereas the peaks for S1c for the charge states < -7 have a higher relative intensity. This bias in ion abundance has previously been attributed to slight differences in the hydrophobicity and the Gibbs free energy of solvatization between nucleotides.[61] The bias observed here is also dependent on the charge state and therefore slight differences in the pK_a values (with S1 < S1c) may also contribute.

Binding Kinetics. Deconvoluted spectra following the binding kinetics of cisplatin to ds1 for up to 50 h in water at a complex-to-oligo nucleotide ratio of 3:1 (equal to approximately 1 platinum per 4 basepairs) are shown in Figure 3. The first observable adduct is the $[Pt(NH_3)_2Cl]^+$ adduct with a mass of 4252.7 and 4181.7 Da for S1 and S1c, respectively. With time these peaks decrease in intensity relative to those corresponding to the bifunctional [Pt-

(58) Bayer, E.; Bauer, T.; Schmeer, K.; Bleicher, K.; Maier, M.; Gaus, H.-J. *Anal. Chem.* **1994**, *66*, 3858–3863.
(59) Wan, K. X.; Gross, M. L.; Shibue, T. *J. Am. Soc. Mass Spectrom.* **2000**, *11*, 450–457.
(60) Gupta, R.; Kapur, A.; Beck, J. L.; Sheil, M. M. *Rapid Commun. Mass Spectrom.* **2001**, *15*, 2472–2480.
(61) Null, A. P.; Nepomuceno, A. I.; Muddiman, D. C. *Anal. Chem.* **2003**, *75*, 1331–339.

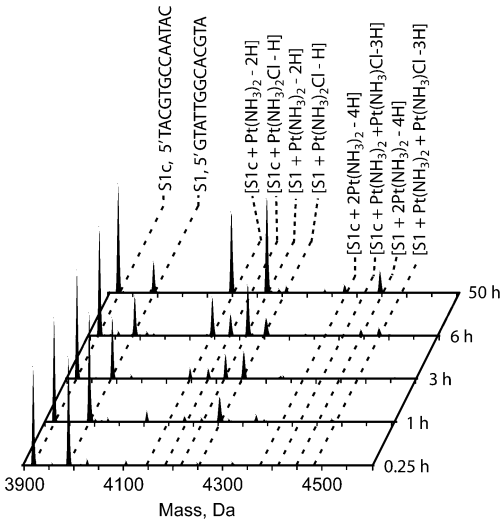

Figure 3. Deconvoluted FT-ICR mass spectra for the reaction of cisplatin with ds1 over time (ds1/cisplatin = 1:3).

$(NH_3)_2]^{2+}$ adducts characterized by peaks centered at 4215.7 and 4144.7 Da, respectively, and further platination affording bis-$Pt(NH_3)_2$ adducts at 4443.7 and 4371.7 Da for S1 and S1c, respectively. Deconvolution over all charge states also eliminates the unequal intensities between the two single-stranded oligonucleotides. It should be noted, however, that deconvolution using ProMass results in loss of the high resolution data. For semiquantitative analysis of the binding kinetics, the intensities of identified adducts at the charge state −6 were used (S1/S1c and S2/S2c were approximately of equal intensity at the start of the incubation; incubation of ds1 and ds2 with cisplatin in a ratio of 1:3; Figure 4). A relative decrease of ca. 60% in the peak height of the signals assigned to the unplatinated single-stranded oligonucleotides of ds1 is reached within 2 h of incubation in the case of S1, but lasted 15 h for the complementary sequence S1c. At thermodynamic equilibrium, which is reached approximately after an incubation period of 15 h, S1 further decreased to less than 3% relative intensity while S1c remained constant at ca. 60%. The faster kinetics as well as the more pronounced decrease of the S1 peaks are possibly a consequence of the presence of the preferred binding sequence (TGGC) in S1, whereas the GTG sequence in S1c represents a less important binding site. Furthermore, S1 contains four guanine residues within its primary sequence, whereas S1c only contains two, and it is therefore expected that S1 is more easily platinated a second time (the bis-$Pt(NH_3)_2$ adduct reaches a maximum relative intensity of approximately 40% for S1, but only 10% for S1c after 50 h).

Overall, the binding of cisplatin takes pace via the formation of a $[Pt(NH_3)_2Cl]^+$ monoadduct, which is transferred ultimately into the final bifunctional $[Pt(NH_3)_2]^{2+}$ adduct. The latter is the most abundant adduct for S1 and S1c at equilibrium (Figure 3). Both types were also observed in ubiquitin-binding studies with cisplatin.[40]

In contrast to ds1, the ds2 oligonucleotide consists of two strands both containing a TGGC-subsequence. However, kinetics and relative peak intensities at equilibrium were not affected by this change in the primary structure and surprisingly led to similar results as the incubation with ds1, where only one strand contained the preferred binding site. While the decrease in relative intensity of S2 is comparable to that of S1 (decrease to ca. 60% within 2 h and to 10% at equilibrium after 15 h), S2c not only decreases at a slower rate than S2, but also remains present with a relative intensity of 80% at equilibrium from 15 h onward. The platination of S2 and S2c with $[Pt(NH_3)_2]^{2+}$ (*m/z* 704.27633 and 687.27709, for $[S2 + Pt(NH_3)_2 - 8\ H]^{6-}$ and $[S2c + Pt(NH_3)_2 - 8\ H]^{6-}$, respectively) takes place in the same manner as for S1 via an intermediate $[Pt(NH_3)_2Cl]^+$ monoadduct (for $[S2 + Pt(NH_3)_2Cl - 7\ H]^{6-}$ and $[S2c + Pt(NH_3)_2Cl - 7\ H]^{6-}$ at *m/z* 710.43891 and 693.43958, respectively). At equilibrium, $[S2c + Pt(NH_3)_2 - 8\ H]^{6-}$ is the most abundant peak, while $[S2 + Pt(NH_3)_2 - 8\ H]^{6-}$ has a relative intensity of ca. 60%, although it is the most abundant S2 containing species. This difference is due to the increased formation of bis-$Pt(NH_3)_2$ adducts in the case of S2 (*m/z* 742.27824), which reach a relative intensity of ca. 30% compared to 10% for S2c (*m/z* 725.11193). As the GG sequences in ds2 are in the closest possible vicinity (due to CCGG subsequence) it can be assumed that, as soon as binding of Pt toward GG in one strand takes place, binding on the complementary strand is (sterically) hindered. Binding kinetics toward S2 is faster than for S2c, which may be due to the higher number of guanosine residues in S2 compared to S2c (5 vs 2, respectively), or due to easier accessibility of GG for cisplatin in S2 than in S2c, and may explain the more pronounced formation of bis-adducts for S2.

Determination of the Preferential Pt Binding Site. FT-ICR MS allows ions to be trapped and fragmented (MS/MS) which can be used to sequence proteins and oligonucleotides via a "top-down" approach. Fragmentation depends on the type of excitation with for example infrared multiphoton dissociation (IRMPD) mainly leading to a/w type fragments.[62] The commonly applied nomenclature for oligonucleotide fragments is summarized in Figure 5.[63] Note that for a n-type fragments usually B_n is lost by an elimination reaction prior to strand breaking due to a second elimination reaction,[64] leading to a furan ring system. Internal fragments, resulting from two strand breaks at the a/w-site, possess a phosphate group at their 5′ terminus, whereas the 3′ terminus carries a furan system.

The 6-fold negatively charged $[Pt(NH_3)_2]^{2+}$ adducts of S1 (containing the GG sequence) and of S1c (containing a GTG sequence) resulting from the incubation of ds1 with cisplatin for 50 h were used for MS/MS studies employing CID and infrared multiphoton dissociation (IRMPD). The energy required to induce fragmentation was increased until a peak of the parent ion was just visible in the tandem mass spectrum. Figure 6 shows the recorded spectra (CID and IRMPD) for the $[S1 + Pt(NH_3)_2 - 8H]^{6-}$ species. Peaks

(62) Hakansson, K.; Hudgins, R. R.; Marshall, A. G.; O'Hair, R. A. J. *J. Am. Soc. Mass Spectrom.* **2003**, *14*, 23–41.
(63) McLuckey, S. A.; Van Berkel, G. J.; Glish, G. L. *J. Am. Soc. Mass Spectrom.* **1992**, *3*, 60–70.
(64) de Hoffmann, E.; Stroobant, V. *Mass Spectrometry: Principles and Applications*, 3rd ed.; John Wiley & Sons: West Sussex, 2007; p 489.

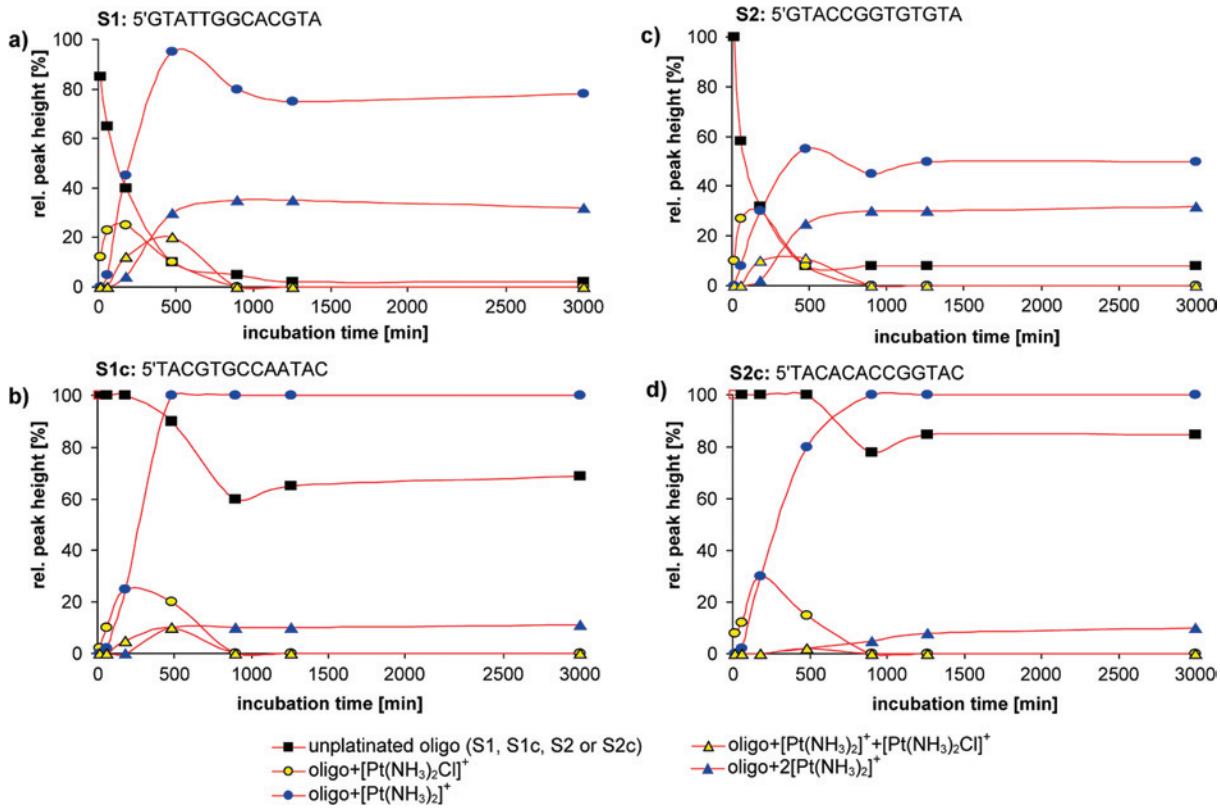

Figure 4. Binding kinetics of cisplatin toward the double-stranded oligonucleotides 5′HO-GTATTGGCACGTA (S1, S1c - ds1) and 5′HO-GTACCGGTGTGTA (S2, S2c - ds2) incubated with cisplatin at an oligonucleotide-to-complex ratio of 1:3. Relative binding kinetics of charge state −6 for S1 and S1c are shown in (a) and (b) and binding kinetics of S2 and S2c are shown in (c) and (d).

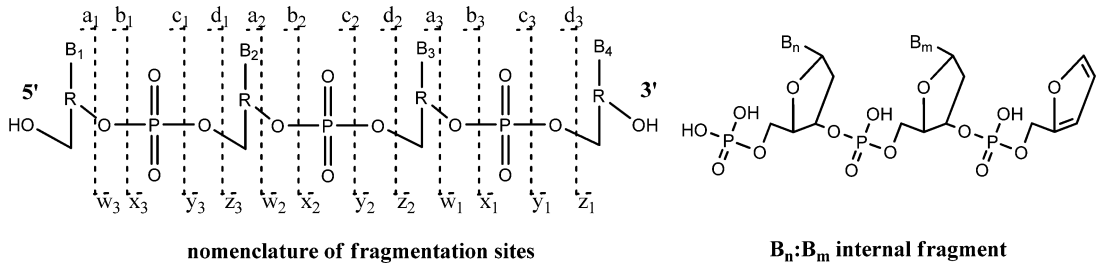

Figure 5. Nomenclature of oligonucleotide fragments observed by tandem MS; a−d fragments correspond to fragments with an intact 5′ terminus and w-z-type fragments have an intact 3′ terminus. Internal fragments resulting from double fragmentation usually occur at the a/w site.

with relative abundances of ≥10% in at least one of the spectra are labeled and assigned to structures. The majority of all assignable peaks originates from $[a_n - B_n]$-type fragments such as $[a_9 - B(A) + Pt(NH_3)_2 - 6H]^{4-}$ (*m*/*z* 705.8529) and w-type fragments such as $[w_{10} + Pt(NH_3)_2 - 7H]^{5-}$ (*m*/*z* 668.89613), and were measured with an accuracy often better than 0.5 ppm with no peak exceeding an inaccuracy of more than 1.5 ppm (see Supporting Information, Table S3 for a complete peak list) for all peaks with a relative intensity >2% and all identified Pt containing fragments of S1. As previously observed in MS studies of oligonucleotides, fragmentation with IRMPD primarily leads to $[a_n - B_n]$ and w-type fragments due to the strong absorption of the phosphate at 10.6 μm, which is typically emitted by the CO_2 laser.[65] CID and IRMPD provided similar fragmentation patterns but with different intensities. Hence, peaks of low relative intensities were often present in only one of the tandem mass spectra.

Assignment of the peaks of >5% relative intensity was almost complete, whereas it was not possible to assign ca. 50% of the platinum-containing peaks with an abundance of <2% (Table S5, Supporting Information). However, the presence of a neighboring peak with a mass difference of 17.0265 Da (loss of the ammine ligand of cisplatin) was used to indicate the presence of a $Pt(NH_3)_2$-containing species, which facilitated the identification of the platinated DNA fragments, especially for low abundant signals (<1% relative intensity) with insufficient isotopic statistics.

The unidentified fragments do not result from a single standard fragmentation pathway (a,b,c,d and w,x,y,z-fragments) nor from internal fragments of the a/w-type. A frequently observed fragment corresponds to a simple base loss (e.g., $[S1 - B(A) + Pt(NH_3)_2 - 8H]^{6-}$ (*m*/*z* 679.10137, relative abundance 40% in CID), and these signals may be

(65) Little, D. P.; Speir, J. P.; Senko, M. W.; O'Connor, P. B.; McLafferty, F. W. *Anal. Chem.* **1994**, *66*, 2809–2815.

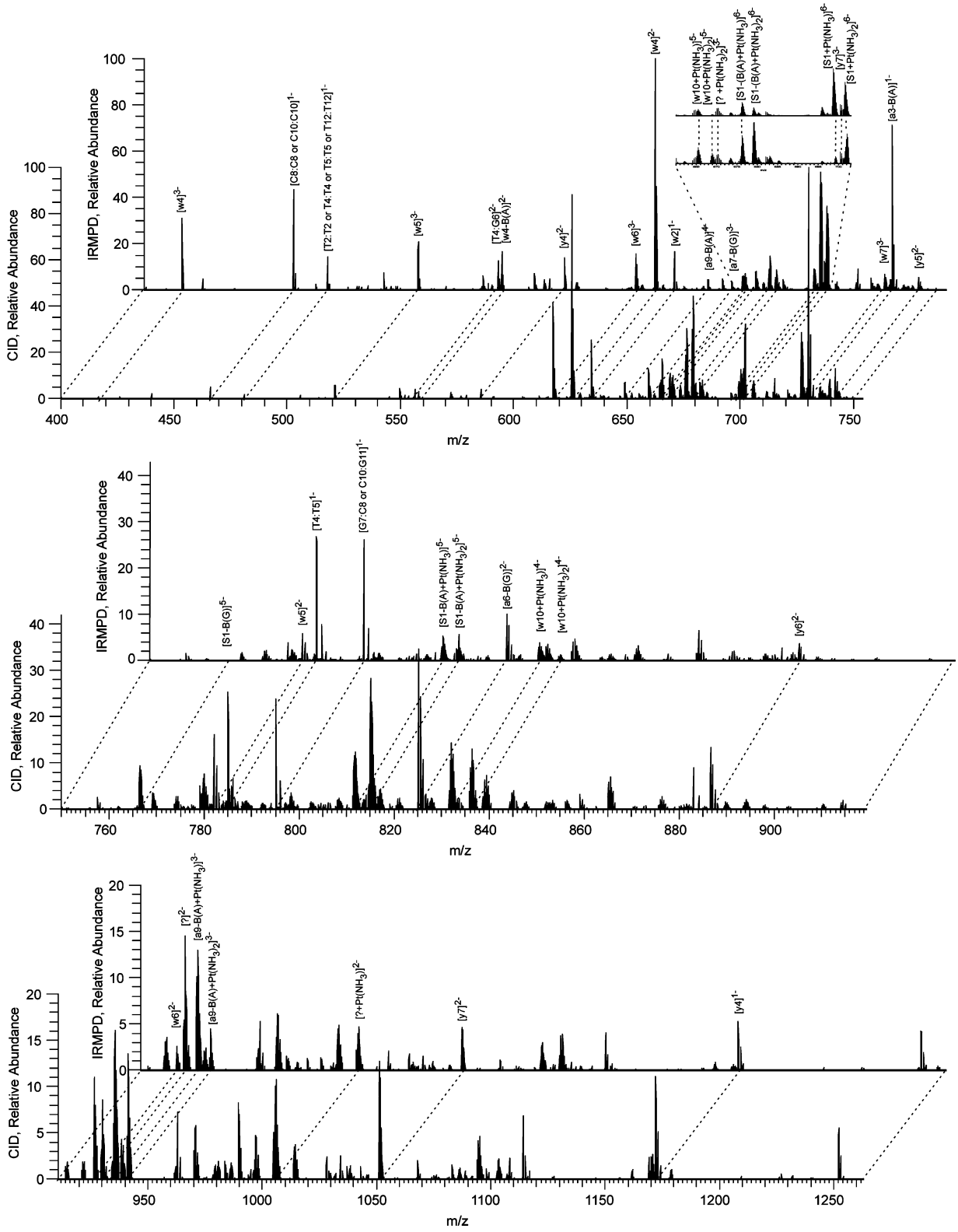

Figure 6. Tandem mass spectra in the mass ranges *m/z* 450−750 (top), 750−920 (middle) and 910−1260 (bottom) of $[S1 + Pt(NH_3)_2 - 8H]^{6-}$ by CID (front) and IRMPD (back). The double-stranded oligonucleotide ds1 was incubated with cisplatin for 50 h and the 6-fold negatively charged platinum monoadduct of S1 was isolated and fragmented (data for the complementary strand S1c is provided in the Supporting Information). All peaks with relative abundance of ≥10% in at least one spectrum are labeled and assigned.

attributed to (one or more) base loss(es) and consecutive strand breaks on a different site in the chain, which result in fragments not covered by the Oligo Mass Calculator. It is worth mentioning that short Pt free fragments (e.g., $[w_2 - H]^{1-}$ at *m/z* 634.10753]), and even short internal fragments (e.g $[T4:T5 - H]^{1-}$ at *m/z* 481.04189 and $[T4:G6 - 2H]^{2-}$ at *m/z* 556.56668) are found in a relative abundance of up to *ca.* 10%, while the much more specific and interesting fragments of short Pt-containing fragments (<5 bases, equals approximately 1800 Da) are rare, and are only present in

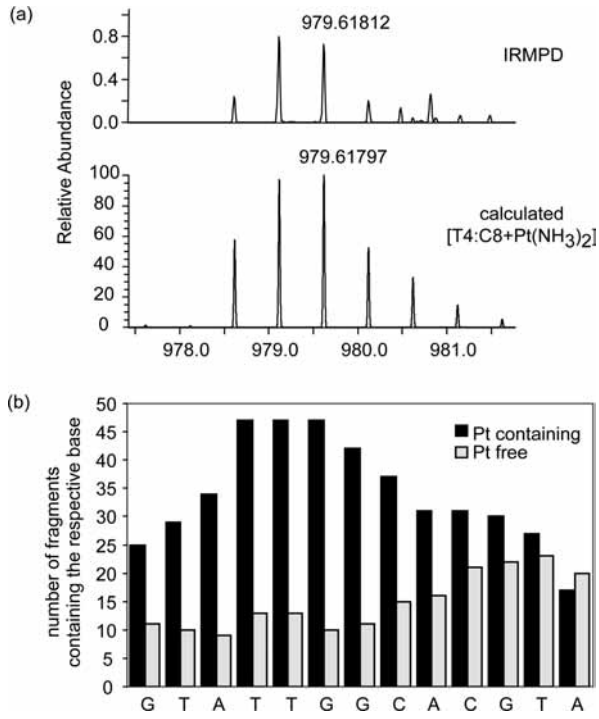

Figure 7. Location of the binding site of cisplatin in S1. (a) The pattern of the smallest assignable Pt-containing fragment $[T4:C8 + Pt(NH_3)_2 - 4H]^{2-}$ resulting from IRMPD fragmentation and the calculated isotopic distribution. (b) Histogram with the occurrence of bases for all assignable Pt-containing as well as Pt-free fragments.

low abundance (<2%). The correct assignment of such peaks is essential for binding site characterization, as the high abundance fragments that contain platinum comprise unspecific, long fragments (w_{10}, base loss, etc.). In S1, the shortest, assignable Pt containing fragment was identified as $[T4:C8 + Pt(NH_3)_2 - 4H]^{2-}$ (*m/z* 979.61812, Figure 7a), and for S1c it was $[a_6 - B(G) + Pt(NH_3)_2 - 4H]^{2-}$ (*m/z* 931.63745). Both are present in low relative abundances of less than 1 and 2%, but cover the expected preferred binding site of cisplatin, namely GG in the case of S1 and GTG in case of S1c. The histogram with the occurrence of bases for all assignable Pt containing fragments further strengthens the T4:C8 region as binding site on S1 (Figure 7b). The TTG-subsequence was most frequently observed in the Pt-containing adducts, providing strong evidence that binding takes place at the GG region, since the affinity of cisplatin to T is low.[28] Furthermore, this binding site coincides with the minimum observed for the Pt-free fragments (Figure 7b).

The complementary strand of S1, that is, S1c, contains the GTG motif, a binding site of secondary importance. Similar to S1, assignment for high abundant peaks was nearly complete, while the low abundant Pt containing fragments are mostly not assigned (the complete peak list of all identified Pt containing peaks in the CID and IRMPD fragmentation experiments and the associated histogram are available in the Supporting Information; Table S4, Figure S1). Small fragments (starting from 1 base in length) were only observed without platinum attached and the smallest assignable Pt-containing fragment, a_6-B(G), contained the expected binding site. A series of large Pt-containing fragments was observed and the peak of the histogram coincides with the GTG-sequence and hence supports the suggested binding site.

The fact that small Pt-containing fragments were not observed in either case is possibly due to the fact that the dicationic platinum adduct, attached to small fragments, neutralizes the negative charge of the phosphate group(s). These small fragments are either neutral or positively charged and hence not detectable.

Conclusions

A FT-ICR MS-based method for the identification of cisplatin/oligonucleotide adducts was not only validated, but also shown to be capable of locating the Pt-binding site via selective fragmentation using CID and IRMPD. FT-ICR MS combines the highest available mass accuracy with advanced MS/MS capabilities and is perfectly suited for studying the interactions of many metal-based anticancer drugs with DNA, the biomolecular target of many metal-based drugs. Binding kinetics are in good agreement with the general accepted mechanisms reported in the literature, with the initial formation of $[Pt(NH_3)Cl]^+$ adducts followed by bifunctional binding of the $[Pt(NH_3)_2]^{2+}$ unit. Both fragmentation techniques, CID and IRMPD, led to similar peak patterns but with different relative intensities, which was found to be especially advantageous for the assignment of low abundant peaks. Statistical analysis of all data allowed the characterization of the preferred binding sites on the oligonucleotides, namely, GG and GTG, confirming those determined by other techniques.[2] Direct determination using FT-ICR MS is limited due to positive charges contributed by coordinated Pt centers being only partly counter-balanced by the negative charges on the smaller oligonucleotide fragments. Nevertheless, this approach for binding site determination is much more rapid than NMR and more generally applicable than X-ray analysis, where a single crystal must be grown, and the bottom-up mass spectrometric approach involving enzymatic digestion of the oligonucleotide in which reactions of the adducts could occur.

Acknowledgment. The authors are indebted to the FFG - Austrian Research Promotion Agency (811591), the Austrian Council for Research and Technology Development (IS526001), the FWF - Austrian Science Fund (P16186-NO3, P18123−N11, P16192-NO3; Schrödinger Fellowship J2613-N19 C.G.H.), the Swiss National Science Foundation and COST D39 (short term scientific mission STSM-D39-3061 A.E.E.).

Supporting Information Available: Details on data processing (internal recalibration and resulting accuracies) for full MS and tandem MS. For S1 a complete peak list of all fragments with an abundance of >2% and all Pt containing fragments with an abundance <2% and for S2 a list with all assignable Pt containing fragments. These lists including measured *m/z* (CID and IRMPD), charge state, assigned adduct neutral sum formula, theoretical *m/z* and accuracy (for CID and IRMPD). The histogram for the location of the binding-site in S1c is shown. This material is available free of charge via the Internet at http://pubs.acs.org.

IC801371R